Polymer Journal (2017) 49, 575–581

www.nature.com/pj

ORIGINAL ARTICLE

Effect of solution viscosity on the production of nanoribbon network hydrogels composed of enzymatically synthesized cellulose oligomers under macromolecular crowding conditions

Yuuki Hata, Toshiki Sawada and Takeshi Serizawa

Cellulose-based hydrogels have gained considerable attention due to their tremendous potential for a wide variety of applications. Recently, we demonstrated the production of nanoribbon network hydrogels through a crystallization-driven self-assembly of cellulose oligomers synthesized by cellodextrin phosphorylase (CDP)-catalyzed reactions under macromolecular crowding conditions. However, the detailed mechanism underlying hydrogel production remains unclear. In this study, we investigated the effect of solution viscosity on hydrogel production by using a highly branched polymer, Ficoll, which created macromolecular crowding conditions with relatively low solution viscosity. The hydrogels were produced through the enzymatic synthesis even in Ficoll solutions. However, greater concentrations of Ficoll were needed for hydrogel production compared with a previously investigated polymer that possessed relatively greater solution viscosity. These observations suggest that a certain level of solution viscosity for the enzymatic synthesis is an essential requirement for hydrogel production.
Polymer Journal (2017) **49,** 575–581; doi:10.1038/pj.2017.22; published online 12 April 2017

INTRODUCTION

Cellulose is a sustainable and abundant raw material that is obtained from natural sources and shows excellent physicochemical properties such as high mechanical strength, chemical stability, biocompatibility and biodegradability.[1–4] In addition to these properties, cellulose has hydrophilic hydroxyl groups abundantly; thus, it has been used for the production of hydrogels with fascinating properties.[5–7] Cellulose-based hydrogels can be obtained through the physical cross-linking of cellulose fiber obtained from plants,[8–10] physical/chemical cross-linking of dissolved cellulose,[11–14] and cultivation of cellulose-producing bacteria.[15,16] These hydrogels have been successfully used for various applications such as scaffolds for cell culture,[8,10,14] supercapacitors,[11] and metal ion adsorbents.[12] Despite their versatile applications, the structural and functional variations of cellulose-based hydrogels are still limited due to the low solubility of cellulose in conventional solvents and the relatively low reactivities of the hydroxyl groups of cellulose. Therefore, it would be beneficial to develop a new methodology to produce cellulose-based hydrogels with designable structures and functions.

The *in vitro* enzymatic synthesis of polymers, such as polypeptides,[17,18] polysaccharides,[19–21] polyesters,[22] and vinyl polymers,[23] is a biomimetic and promising approach to produce functional polymer materials with unique structural properties.[24] For example, it has been reported that two-dimensional rectangular nanoassemblies can be obtained as precipitates through crystallization-driven self-assembly of cellulose oligomers synthesized by the CDP-catalyzed reverse phosphorolysis reaction using α-D-glucose 1-phosphate (αG1P) monomers and D-glucose primers in a single step under mild aqueous conditions.[25,26] In the nanoassemblies, cellulose oligomers with an average degree of polymerization (DP) of 10 aligned perpendicularly to the base plane, forming a lamellar crystal with the cellulose II allomorph.[26] Furthermore, we have recently demonstrated that when D-glucose derivatives with azide,[27] alkyl,[28] and oligo(ethylene glycol) groups[29] were used as primers for the CDP-catalyzed reaction, functional nanoassemblies composed of cellulose oligomer derivatives were produced. More recently, we demonstrated nanoribbon network hydrogels produced through the CDP-catalyzed synthesis of cellulose oligomers under macromolecular crowding conditions, which were prepared using concentrated aqueous solutions of dextran (Dex), poly(ethylene glycol) and poly(*N*-vinylpyrrolidone).[30] In general, macromolecular crowding increases solution viscosity to decrease the diffusion rates of colloids[31] and induces excluded volume effects to generate depletion repulsion between colloids within a certain time period.[32] For these possible reasons, the aggregation of the two-dimensional nanoassemblies appeared to be suppressed, leading to further growth into the nanoribbon networks for hydrogel production. However, the essential factors underlying hydrogel

Department of Chemical Science and Engineering, School of Materials and Chemical Technology, Tokyo Institute of Technology, Tokyo, Japan
Correspondence: Professor T Serizawa, Department of Chemical Science and Engineering, School of Materials and Chemical Technology, Tokyo Institute of Technology, 2-12-1-H121 Ookayama, Meguro-ku, Tokyo 152-8550, Japan.
E-mail: serizawa@polymer.titech.ac.jp
Received 17 February 2017; revised 16 March 2017; accepted 17 March 2017; published online 12 April 2017

production under macromolecular crowding conditions remain unclear. Therefore, it is necessary to analyze the plausible factors for hydrogel production individually.

Among water-soluble polymers for the preparation of macromolecular crowding, a highly branched polysaccharide, Ficoll, which is synthesized through the copolymerization of sucrose and epichlorohydrin, creates macromolecular crowding with relatively low solution viscosity.[31,33,34] Therefore, Ficoll solutions are useful to analyze the contribution of solution viscosity to macromolecular crowding systems. In this study, the effect of solution viscosity on the production of nanoribbon network hydrogels composed of enzymatically synthesized cellulose oligomers was investigated using Ficoll solutions (Figure 1). The hydrogels were produced in Ficoll solutions; however, greater concentrations of Ficoll were needed compared to Dex, which has higher solution viscosity, suggesting that a certain level of solution viscosity is an essential requirement for hydrogel production.

EXPERIMENTAL PROCEDURES

Materials

αG1P disodium salt *n*-hydrate, 40% sodium deuteroxide (NaOD)/deuterium oxide (D_2O) solution and Dex (150 kDa) were purchased from Wako Pure Chemical Industries (Osaka, Japan). Ficoll (PM70), ProteoMass MALDI-MS Standard, 1% trifluoroacetic acid, acetonitrile, 2,5-dihydroxybenzoic acid and D_2O were purchased from Sigma-Aldrich (Tokyo, Japan). Dotite was purchased from Nisshin EM Corporation (Tokyo, Japan). All of the other reagents were purchased from Nacalai Tesque (Kyoto, Japan). Ultrapure water with resistivity greater than 18.2 MΩ cm was obtained from a Milli-Q Advantage A-10 (Merck Millipore, Darmstadt, Germany) and was used for all the experiments.

CDP-catalyzed synthesis of cellulose oligomers under macromolecular crowding conditions

CDP preparation and CDP-catalyzed synthesis of cellulose oligomers under macromolecular crowding conditions were performed according to our previously reported protocols.[26,30] Briefly, CDP from *Clostridium thermocellum* YM4 was prepared in *Escherichia coli* BL21-Gold (DE3) harboring plasmid pET28a-CDP cultures and then purified using a Ni-NTA column (GE Healthcare, Tokyo, Japan). CDP (0.2 U ml^{-1}) was incubated with αG1P (0.2 M) and D-glucose (0.05 M) in 4-(2-hydroxyethyl)-1-piperazineethanesulfonic acid buffer solution (0.5 M, pH 7.5) containing Ficoll or Dex (2, 5, 10, or 20% (w/v)) at 60 °C for 3 days. The products were observed by optical microscopy immediately after the reactions. For scanning electron microscopy (SEM) observations, the gelled products were purified by immersion in ultrapure water at 4 °C for at least 1 week. The ultrapure water was exchanged each day. For other analyses, the gelled and precipitated products were collapsed mechanically by using water flow to obtain water-dispersed products. The products were washed with ultrapure water through centrifugation (15 000 r.p.m)/redispersion cycles to remove 99.999% of the reaction mixture. The purified products were stored at 4 °C immediately after the purification or after the subsequent lyophilization.

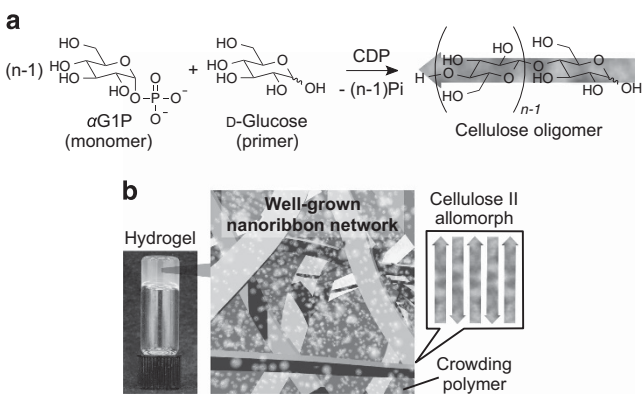

Figure 1 (**a**) Synthetic scheme of cellulose oligomers via CDP-catalyzed oligomerizations of αG1P monomers from D-glucose primers. (**b**) Schematic illustration of the resulting hydrogels composed of well-grown nanoribbon networks with the cellulose II allomorph.

Solution viscosity measurements

The viscosity of the reaction mixtures containing Ficoll or Dex before the enzymatic reaction was measured using a viscometer (SV-1A, A&D, Tokyo, Japan) at 60 °C. Note that CDP was not added into the reaction mixtures for solution viscosity measurements to avoid progress in the enzymatic reactions. CDP was considered to have a negligible effect on the viscosity of the reaction mixtures due to its relatively small concentration (6 mg l^{-1} based on absorbance at 280 nm).[35]

Compression tests

Cylinder-shaped hydrogels with a diameter of 15 mm and a height of 7.5 mm were prepared in the presence of 20% (w/v) Ficoll using a Teflon mold. The hydrogels were applied to compression tests immediately after the preparation. The compression tests were carried out using a Shimadzu AGS-X at a velocity of 2 mm min^{-1}. Young's modulus was determined by the average slope over the strain ratio range of 0–0.05 from the stress–strain curve and presented as the average of five individual trials.

^{1}H nuclear magnetic resonance (NMR) spectroscopy

The lyophilized products were dissolved in 4% NaOD/D_2O to prepare product solutions (⩾2% (w/v)). ^{1}H NMR spectra of the product solutions were recorded on an AVANCE III HD500 (Bruker Biospin, Yokohama, Japan, 500 MHz) at ambient temperature. Residual signals of water were used as an internal standard ($\delta = 4.79$) to calibrate the spectra.

Matrix-assisted laser desorption/ionization time-of-flight mass spectrometry (MALDI-TOF-MS)

The product dispersions (0.0033% (w/v)) containing 2,5-dihydroxybenzoic acid (1.7 mg ml^{-1}), trifluoroacetic acid (0.02% (v/v)) and acetonitrile (50% (v/v)) were prepared from the water dispersions and then deposited onto a sample target plate to prepare measurement samples. The samples were measured at an accelerating potential of 20 kV in linear-positive ion mode using a Shimadzu (Kyoto, Japan) AXIMA-performance mass spectrometer equipped with a nitrogen laser ($\lambda = 337$ nm) and pulsed ion extraction. The spectra were calibrated using peptide standards (ProteoMass MALDI-MS Standard) at 757.3997 Da (Bradykinin fragment 1–7), 1533.8582 Da ($P_{14}R$) and 2465.1989 Da (ACTH fragment 18–39).

Wide-angle X-ray diffraction (WAXD) measurements

WAXD profiles of the lyophilized products in a powdery state were measured under ambient conditions using a Rigaku (Tokyo, Japan) MiniFlex600 with Cu Kα radiation ($\lambda = 1.54$ Å). The profiles were collected in the 2θ range of 5–40° with a step of 0.02° at a scan speed of 2° min^{-1} at ambient temperature.

Attenuated total reflection-Fourier transform infrared (ATR-FTIR) absorption spectroscopy

ATR-FTIR absorption spectra of the lyophilized products in a powdery state were measured using a JASCO (Tokyo, Japan) FT/IR-4100 spectrometer with a cumulative number of 100 and a resolution of 2.0 cm^{-1} at ambient temperature.

SEM observations

The water solvent of the purified hydrogels was exchanged by immersing the hydrogels stepwise in 10, 20, 30, 40, 50, 60, 70, 80 and 90% ethanol, ethanol, ethanol/*tert*-butyl alcohol (50:50), and *tert*-butyl alcohol. The resultant organogels were rapidly frozen using liquid nitrogen, fractured using a razor blade and then lyophilized. Note that the volumes of the gels were almost the same before and after solvent exchange. The resultant xerogels were mounted

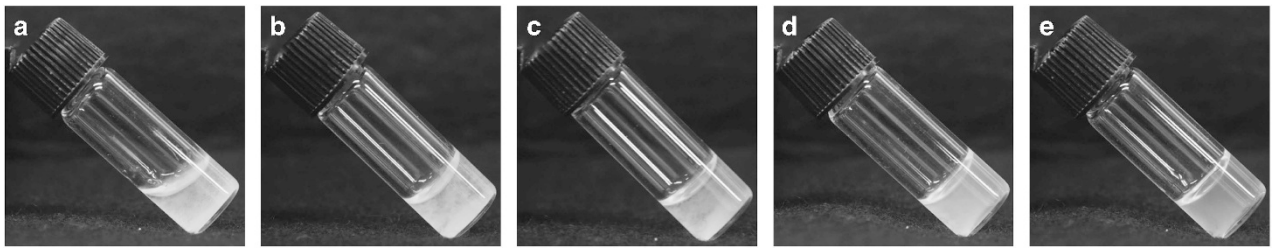

Figure 2 Images of the reaction mixtures after 3 days of incubation (**a**) in the absence or presence of (**b**) 2% (w/v), (**c**) 5% (w/v), (**d**) 10% (w/v) and (**e**) 20% (w/v) Ficoll.

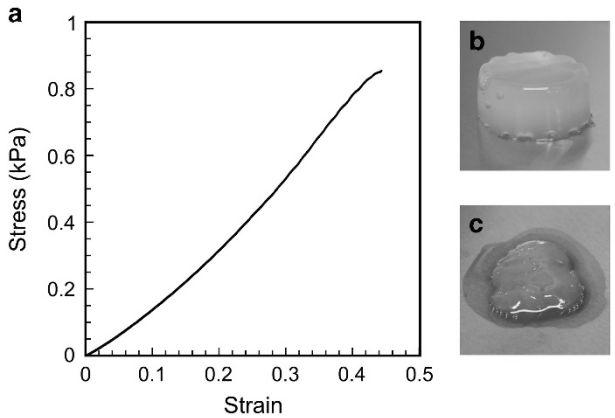

Figure 3 (**a**) Compressive stress–strain curve of the hydrogels prepared in the presence of 20% (w/v) Ficoll. Images of the hydrogels applied to the tests: (**b**) before and (**c**) after compression. A full color version of this figure is available at the *Polymer Journal* online.

on substrates with Dotite and then coated with osmium. SEM images of the xerogels prepared in the presence of 10 and 20% (w/v) Ficoll were obtained on field-emission scanning electron microscopes (S-4700, Hitachi High-Technologies, Tokyo, Japan; JSM-7500F, JEOL, Tokyo, Japan) at accelerating voltages of 6 and 5 kV, respectively.

Atomic force microscopy (AFM)

The water dispersions of the products (0.001% (w/v)) were spin-cast on mica substrates at 600 r.p.m. for 30 min. The samples were observed using a Shimadzu (Kyoto, Japan) SPM-9600 in tapping mode at ambient temperature.

Optical microscopy

The 2-mm-thick hydrogels produced in 96-well microplates were observed using a ZOE Fluorescent Cell Imager (Bio-Rad, Tokyo, Japan) at ambient temperature. The images were subjected to thresholding by using ImageJ to obtain binary images.

RESULTS AND DISCUSSION

Enzymatic synthesis of cellulose oligomers in Ficoll solutions

Before the enzymatic synthesis, the solution viscosities of the reaction mixtures containing 10% (w/v) and 20% (w/v) Ficoll were measured to be 2.8 ± 0.1 mPa s and 7.9 ± 0.2 mPa s, respectively. The former value was clearly lower than that of the solution containing 10% (w/v) Dex (8.4 ± 0.2 mPa s). Thus, reaction mixtures with lower solution viscosities were successfully prepared by using highly branched Ficoll as a crowding polymer. When cellulose oligomers were enzymatically synthesized in 0, 2, 5, 10 and 20% (w/v) Ficoll solutions, the colorless products were observed in all the solutions, suggesting the successful synthesis of water-insoluble cellulose oligomers even in the presence of Ficoll (Figure 2). Although the products synthesized without Ficoll were observed as precipitates on the internal surface of a reaction glass vial, the apparent volume of the products gradually increased with increasing Ficoll concentrations. Finally, the entirety of the reaction mixtures was transformed into opaque hydrogels at 10 and 20% (w/v) Ficoll. These observations indicated that hydrogels were also produced by the enzymatic synthesis in Ficoll solutions, and that macromolecular crowding conditions were essential for hydrogel production based on suppression of aggregation/precipitation of the product. In our previous report, we revealed that the minimum concentration of Dex for hydrogel production was 5% (w/v).[30] Thus, the enzymatic synthesis in the presence of Ficoll required greater polymer concentrations for hydrogel production than in the presence of Dex, suggesting that a certain level of solution viscosity is required for hydrogel production.

The product amounts were estimated to be 2.0, 1.9, 1.5 and 1.2 mg collected from the 200 μl reaction mixtures in the presence of 2, 5, 10 and 20% (w/v) Ficoll, respectively. The conversions of αG1P monomers were estimated to be ~25, 25, 20 and 15%, respectively, based on the average DP of the products (see below). The monomer conversion without crowding polymers has been reported to be 35%;[26] therefore, the monomer conversions tended to decrease with increasing Ficoll concentrations. In our previous report, we revealed that the monomer conversions for the reactions in the presence of crowding polymers were also lower than in the absence of crowding polymers.[30] The decrease in the monomer conversions was attributed to the influences of macromolecular crowding conditions, such as high solution viscosities,[36] changes in water activities,[37] and/or changes in the dielectric constant of water solvents [38] on the enzymatic reactions.

The cylinder-shaped hydrogels (diameter: 15 mm; thickness: 7.5 mm) prepared in the presence of 20% (w/v) Ficoll were applied to compression tests. The stress − strain curves revealed that the hydrogels showed the Young's modulus of 1240 ± 160 Pa (Figure 3a). This value was slightly larger than that of the hydrogels prepared in the presence of 10% (w/v) Dex despite the smaller monomer conversion,[30] suggesting that network structures of the hydrogels varied depending on the crowding polymers and/or their concentrations. After the compression, water solvent was forced out of the hydrogels, suggesting a sponge-like porous structure of the hydrogels (Figure 3b and c). Accordingly, we found that the enzymatic synthesis of cellulose oligomers under macromolecular crowding conditions prepared by Ficoll produced hydrogels, similarly to other crowding polymers.[30]

Chemical structural characterization of the products

The products were dissolved in 4% NaOD/D_2O for ^{1}H NMR spectroscopic analyses. ^{1}H NMR spectra of the product solutions showed signals assignable to the protons of cellulose oligomers (Figure 4).[39–41] Notably, proton signals for crowding polymers were not observed, indicating that the purification process was successful.

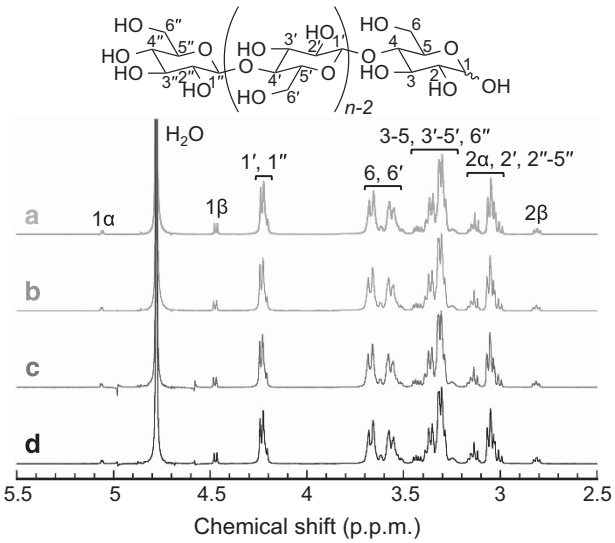

Figure 4 NMR spectra of the products prepared in the presence of (**a**) 2% (w/v), (**b**) 5% (w/v), (**c**) 10% (w/v) and (**d**) 20% (w/v) Ficoll.

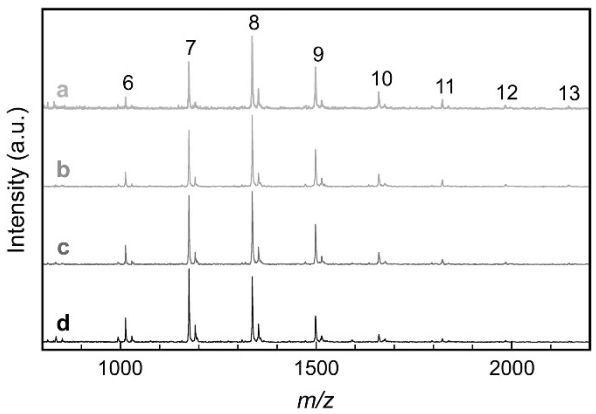

Figure 5 MALDI-TOF-MS of the products prepared in the presence of (**a**) 2% (w/v), (**b**) 5% (w/v), (**c**) 10% (w/v) and (**d**) 20% (w/v) Ficoll.

On the basis of the integral ratios for the signals of $H_{1\alpha}$ ($\delta = 5.1$), $H_{1\beta}$ ($\delta = 4.5$) and $H_{1',1''}$ ($\delta = 4.3$), the average DPs of the cellulose oligomers were calculated to be 9, 8, 8 and 8 for the enzymatic reactions in the presence of 2, 5, 10 and 20% (w/v) Ficoll, respectively. These values were slightly lower than that for the reaction without crowding polymers (that is, 10)[26] and tended to decrease with increasing Ficoll concentrations. It is known that the chain growth of cellulose oligomers is terminated by their crystallization when the molecular chain has grown sufficiently long to become water-insoluble.[25,42] Therefore, the decrease in the average DP indicated that cellulose oligomers with relatively smaller DPs crystallized in the reaction mixtures crowded with Ficoll. In general, under macromolecular crowding conditions, colloids disperse stably within a certain time period due to depletion repulsion,[32] and intermolecular interactions change due to changes in the physicochemical properties of the water solvents.[43] Therefore, collision frequencies between the synthesized cellulose oligomers and the colloidal product might be increased, and/or interactions between cellulose oligomers might be promoted, leading to crystallization of the molecular chains with smaller DPs. The average DP of cellulose oligomers synthesized in the presence of 10% (w/v) and 20% (w/v) Ficoll (that is, 8) was slightly

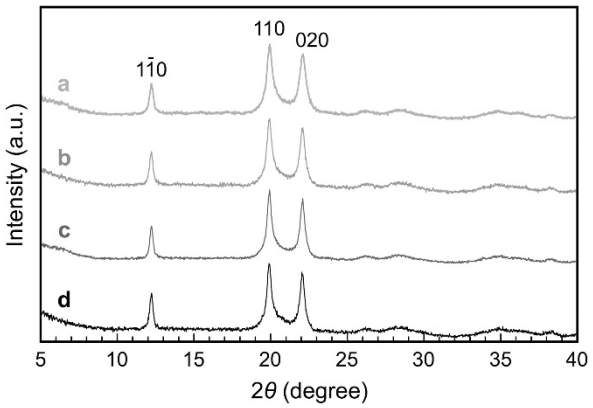

Figure 6 WAXD profiles of the products prepared in the presence of (**a**) 2% (w/v), (**b**) 5% (w/v), (**c**) 10% (w/v) and (**d**) 20% (w/v) Ficoll.

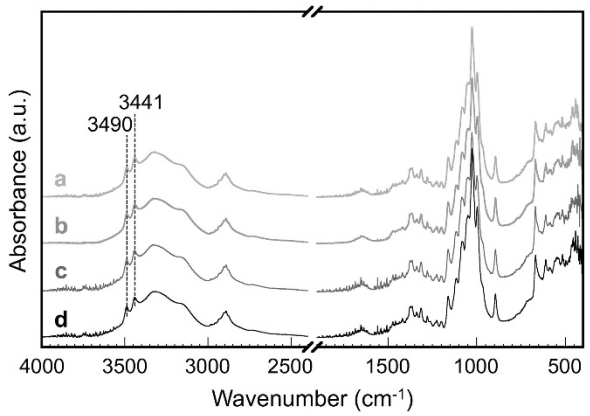

Figure 7 ATR-FTIR absorption spectra of the products prepared in the presence of (**a**) 2% (w/v), (**b**) 5% (w/v), (**c**) 10% (w/v) and (**d**) 20% (w/v) Ficoll.

smaller than that of the oligomers synthesized in the presence of 10% (w/v) Dex (that is, 9),[30] suggesting that the contribution of crowding polymers to the DP is variable depending on polymer characteristics.

The chemical structures of the products synthesized in the presence of 2, 5, 10 and 20% (w/v) Ficoll were further characterized by MALDI-TOF-MS. All of the mass spectra showed two series of peaks with peak-to-peak mass differences of 162 Da, corresponding to a single glucosyl unit (Figure 5). The *m/z* values of the two series of peaks corresponded to cellulose oligomers with sodium and potassium ion adducts, respectively, confirming that the enzymatic synthesis of cellulose oligomers successfully proceeded even in the presence of Ficoll. The DPs ranged approximately from 6 to 13. The DP of the peak with maximum intensity decreased with increasing Ficoll concentrations, further supporting cellulose oligomers with relatively smaller DPs having crystallized during the reactions.

Characterization of the crystal structures formed by the products

The WAXD profiles of the products showed peaks for *d*-spacings of 0.72, 0.45 and 0.40 nm, regardless of the Ficoll concentration (Figure 6). The peaks were attributed to the 1$\bar{1}$0, 110 and 020 diffractions of the cellulose II allomorph for anti-parallel alignment, respectively.[25] In addition, the ATR-FTIR absorption spectra of the products showed two sharp peaks at approximately 3441 and 3490 cm^{-1}, which were attributed to the 2-OH···O-6 intramolecular

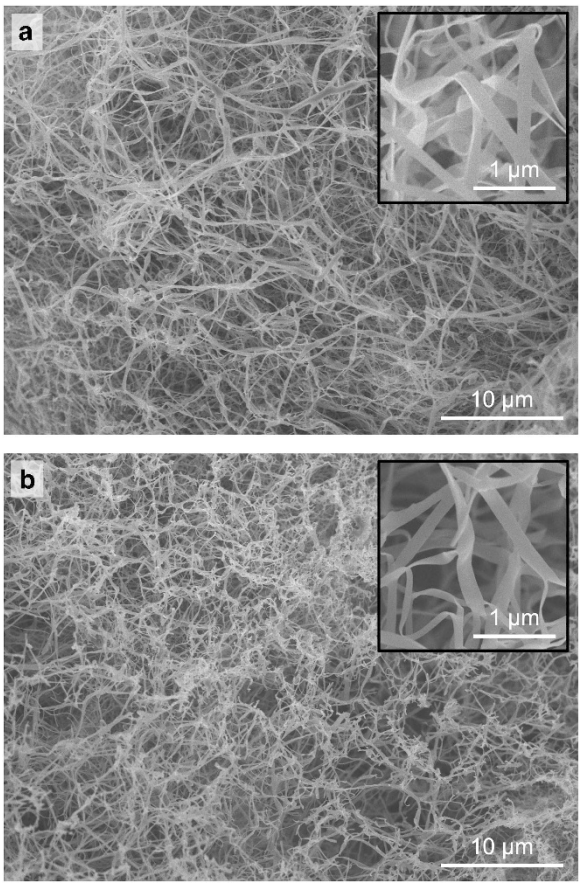

Figure 8 SEM images of the xerogels prepared in the presence of (**a**) 10% (w/v) and (**b**) 20% (w/v) Ficoll. Insets show magnified images.

hydrogen bonds for the cellulose II allomorph (Figure 7).[44] These results revealed that the cellulose molecules in the products were in the cellulose II allomorph. The crystal structures were the same as the products synthesized in the presence[30] or absence[25,26] of crowding polymers, indicating that Ficoll did not affect the crystal structures of the synthesized cellulose oligomers.

Morphological characterization of the hydrogel network structures

To reveal the morphologies of the hydrogel network structures, the hydrogels prepared in the presence of 10% (w/v) and 20% (w/v) Ficoll were observed by SEM and AFM. The SEM images of the xerogels prepared by lyophilization of the hydrogels after the removal of Ficoll revealed well-grown networks composed of nanoribbons with a width of several hundred nanometers (Figure 8). Notably, there was no branching of the nanoribbons, as far as we examined them. These morphologies were similar to that of the hydrogels produced in the presence of Dex.[30] AFM observations for the mechanically crushed nanoribbons prepared in the presence of 10% (w/v) revealed a thickness of 5.1 ± 0.4 nm (Figure 9a), which was comparable to the chain length of cellulose oligomers with a DP of 8 (4.2 nm, Figure 9b). Therefore, the molecular chains appeared to align perpendicularly to the base plane of the nanoribbons to form a lamellar crystal, similar to the cellulose chains in two-dimensional rectangular nanoassemblies produced without crowding polymers.[25,26] Taking the characterizations together, it appeared that the two-dimensional rectangular cellulose nanoassemblies grew into nanoribbon networks without

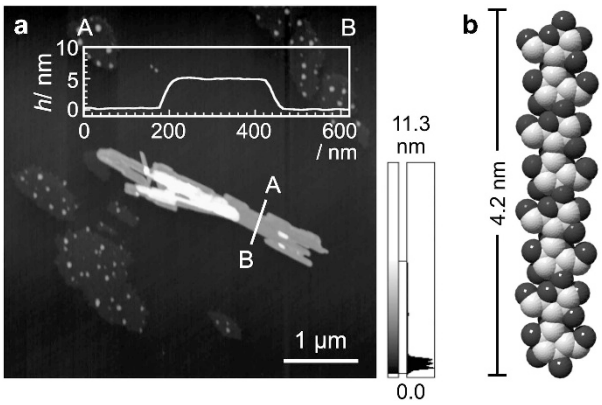

Figure 9 (**a**) AFM image of the nanoribbons from the hydrogel prepared in the presence of 10% (w/v) Ficoll. Inset shows a cross-sectional height profile. (**b**) A CPK model of cellooctaose (DP = 8) in the cellulose II allomorph.

aggregation/precipitation under macromolecular crowding conditions prepared even with Ficoll.

Macroscopic characterization of the nanoribbon network hydrogels

Optical microscopy was used to evaluate the macroscopic distribution of the nanoribbon networks in the hydrogels. The optical microscopy image of the hydrogels prepared in the presence of 10% (w/v) Ficoll showed regions where the image was distinctly out of focus (Figure 10a), whereas the image prepared in the presence of 20% (w/v) Ficoll was in focus throughout (Figure 10b). This result suggested that the nanoribbon networks prepared in the presence of 10% (w/v) Ficoll were relatively non-uniform at the macroscopic level compared with that prepared in the presence of 20% (w/v) Ficoll. When the optical images were binary processed, the non-uniformity of the former hydrogels was observed more clearly (Figure 10a, inset). The non-uniformity of the nanoribbon networks represents a certain level of aggregation of the nanoribbons. The hydrogels prepared in the presence of 20% (w/v) Ficoll were similar to those prepared in the presence of 10% (w/v) Dex (Figure 10c). Note that the solution viscosity of 20% (w/v) Ficoll and 10% (w/v) Dex solutions are similar. Therefore, these observations strongly suggested that a certain level of solution viscosity under macromolecular crowding conditions was essential to produce more uniform nanoribbon networks at the macroscopic level.

CONCLUSION

We investigated the effect of solution viscosity on the production of nanoribbon network hydrogels composed of cellulose oligomers enzymatically synthesized under macromolecular crowding conditions. A highly branched polymer, Ficoll, was used to create the conditions with relatively low solution viscosity. The hydrogels were produced through the CDP-catalyzed reactions even in Ficoll solutions, similarly to in Dex solutions with higher solution viscosity. However, the minimum concentrations of Ficoll required for the production of uniform hydrogels were greater than those of Dex. Thus, we revealed that a certain level of solution viscosity was needed to produce well-grown nanoribbon networks, suggesting solution viscosity to be an essential factor for hydrogel production. Recently, we reported that D-glucose derivatives with azide,[27] alkyl,[28] and oligo (ethylene glycol) groups[29] were recognized by CDP as primers to enzymatically produce functional nanoassemblies composed of cellulose oligomer derivatives. The enzymatic synthesis using these primers

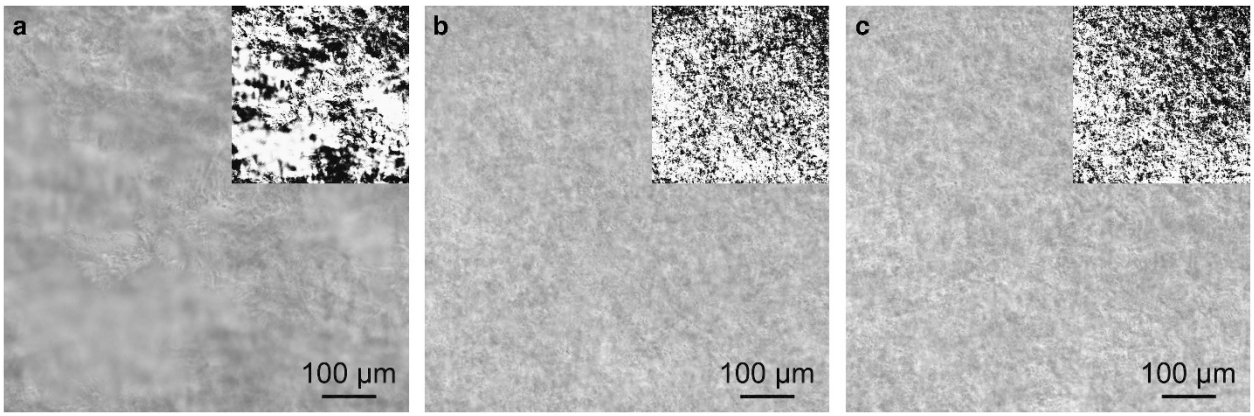

Figure 10 Optical microscopy images of the hydrogel prepared in the presence of (**a**) 10% (w/v) FicoII, (**b**) 20% (w/v) FicoII and (**c**) 10% (w/v) Dex. Insets represent binary images from the optical microscopy images.

under macromolecular crowding conditions has the potential to produce nanoribbon network hydrogels with diverse functions. The cellulose-based hydrogels will have a wide variety of applications particularly in biomedical fields. As a consequence, our findings will help to open a new avenue for the production of unprecedented cellulose-based hydrogels with unique nanostructures and tailored functions.

CONFLICT OF INTEREST

The authors declare no conflict of interest.

ACKNOWLEDGEMENTS

The authors wish to thank Prof J. Watanabe and Prof M. Tokita (Tokyo Tech) for solution viscosity measurements and the Division of Materials Analysis Ookayama (Tokyo Tech) for SEM observations and WAXD measurements. This study was partially supported by the Funding Program for Next Generation World-Leading Researchers (NEXT Program, GR022), the Grants-in-Aids for Scientific Research (26288056, 26620174 and 16K14075) from the Japan Society for the Promotion of Science, and the collaborative research with JX Nippon Oil & Energy Corporation.

1 Klemm, D., Heublein, B., Fink, H.-P. & Bohn, A. Cellulose: fascinating biopolymer and sustainable raw material. *Anegw. Chem. Int. Ed.* **44**, 3358–3393 (2005).
2 Habibi, Y., Lucia, L. A. & Rojas, O. J. Cellulose nanocrystals: chemistry, self-assembly, and applications. *Chem. Rev.* **110**, 3479–3500 (2010).
3 Klemm, D., Kramer, F., Moritz, S., Lindström, T., Ankerfors, M., Gray, D. & Dorris, A. Nanocelluloses: a new family of nature based materials. *Anegw. Chem. Int. Ed.* **50**, 5438–5466 (2011).
4 Moon, R. J., Martini, A., Nairn, J., Simonsen, J. & Youngblood, J. Cellulose nanomaterials review: structure, properties and nanocomposites. *Chem. Soc. Rev.* **40**, 3941–3994 (2011).
5 Sannino, A., Demitri, C. & Madaghiele, M. Biodegradable cellulose-based hydrogels: design and applications. *Materials* **2**, 353–373 (2009).
6 Chang, C. & Zhang, L. Cellulose-based hydrogels: present status and application prospects. *Carbohydr. Polym.* **84**, 40–53 (2011).
7 Shen, X., Shamshina, J. L., Berton, P., Gurau, G. & Rogers, R. D. Hydrogels based on cellulose and chitin: fabrication, properties, and applications. *Green Chem.* **18**, 53–75 (2016).
8 Bhattacharya, M., Malinen, M. M., Lauren, P., Lou, Y.-R., Kuisma, S. W., Kanninen, L., Lille, M., Corlu, A., GuGuen-Guillouzo, C., Ikkala, O., Laukkanen, A., Urtti, A. & Yliperttula, M. Nanofibrillar cellulose hydrogel promotes three-dimensional liver cell culture. *J. Control. Release* **164**, 291–298 (2012).
9 Dong, H., Snyder, J. F., Williams, K. S. & Andzelm, J. W. Cation-induced hydrogels of cellulose nanofibrils with tunable moduli. *Biomacromolecules* **14**, 3338–3345 (2013).
10 Zander, N. E., Dong, H., Steele, J. & Grant, J. T. Metal cation cross-linked nanocellulose hydrogels as tissue engineering substrates. *ACS Appl. Mater. Interfaces* **6**, 18502–18510 (2014).
11 Ouyang, W., Sun, J., Memon, J., Wang, C., Geng, J. & Huang, Y. Scalable preparation of three-dimensional porous structures of reduced graphene oxide/cellulose composites and their application in supercapacitors. *Carbon* **62**, 501–509 (2013).
12 Isobe, N., Chen, X., Kim, U.-J., Kimura, S., Wada, M., Saito, T. & Isogai, A. TEMPO-oxidized cellulose hydrogel as a high-capacity and reusable heavy metal ion adsorbent. *J. Hazard. Mater.* **260**, 195–201 (2013).
13 Zhao, D., Huang, J., Zhong, Y., Li, K., Zhang, L. & Cai, J. High-strength and high-toughness double-cross-linked cellulose hydrogels: a new strategy using sequential chemical and physical cross-linking. *Adv. Funct. Mater.* **26**, 6279–6287 (2016).
14 Xu, D., Fan, L., Gao, L., Xiong, Y., Wang, Y., Ye, Q., Yu, A., Dai, H., Yin, Y., Cai, J. & Zhang, L. Micro-nanostructured polyaniline assembled in cellulose matrix via interfacial polymerization for applications in nerve regeneration. *ACS Appl. Mater. Interfaces* **8**, 17090–17097 (2016).
15 Gatenholm, P. & Klemm, D. Bacterial nanocellulose as a renewable material for biomedical applications. *MRS Bull.* **35**, 208–213 (2010).
16 Fu, L., Zhang, J. & Yang, G. Present status and applications of bacterial cellulose-based materials for skin tissue repair. *Carbohydr. Polym.* **92**, 1432–1442 (2013).
17 Numata, K. Poly(amino acid)s/polypeptides as potential functional and structural materials. *Polym. J.* **47**, 537–545 (2015).
18 Nitta, S., Komatsu, A., Ishii, T., Iwamoto, H. & Numata, K. Synthesis of peptides with narrow molecular weight distributions via exopeptidase-catalyzed aminolysis of hydrophobic amino-acid alkyl esters. *Polym. J.* **48**, 955–961 (2016).
19 Kobayashi, S., Sakamoto, J. & Kimura, S. *In vitro* synthesis of cellulose and related polysaccharides. *Prog. Polym. Sci.* **26**, 1525–1560 (2001).
20 Kadokawa, J. Precision polysaccharide synthesis catalyzed by enzymes. *Chem. Rev.* **111**, 4308–4345 (2011).
21 Nishimura, T. & Akiyoshi, K. Amylose engineering: phosphorylase-catalyzed polymerization of functional saccharide primers for glycobiomaterials. *WIREs Nanomed. Nanobiotechnol.* **9**, e1423 (2017).
22 Takeoka, Y., Hayashi, M., Sugiyama, N., Yoshizawa-Fujita, M., Aizawa, M. & Rikukawa, M. *In situ* preparation of poly(L-lactic acid-*co*-glycolic acid)/hydroxyapatite composites as artificial bone materials. *Polym. J.* **47**, 164–170 (2015).
23 Kohri, M. Development of HRP-mediated enzymatic polymerization under heterogeneous conditions for the preparation of functional particles. *Polym. J.* **46**, 373–380 (2014).
24 Shoda, S., Uyama, H., Kadokawa, J., Kimura, S. & Kobayashi, S. Enzymes as green catalysts for precision macromolecular synthesis. *Chem. Rev.* **116**, 2307–2413 (2016).
25 Hiraishi, M., Igarashi, K., Kimura, S., Wada, M., Kitaoka, M. & Samejima, M. Synthesis of highly ordered cellulose II *in vitro* using cellodextrin phosphorylase. *Carbohydr. Res.* **344**, 2468–2473 (2009).
26 Serizawa, T., Kato, M., Okura, H., Sawada, T. & Wada, M. Hydrolytic activities of artificial nanocellulose synthesized via phosphorylase-catalyzed enzymatic reactions. *Polym. J.* **48**, 539–544 (2016).
27 Yataka, Y., Sawada, T. & Serizawa, T. Enzymatic synthesis and post-functionalization of two-dimensional crystalline cellulose oligomers with surface-reactive groups. *Chem. Commun.* **51**, 12525–12528 (2015).
28 Yataka, Y., Sawada, T. & Serizawa, T. Multidimensional self-assembled structures of alkylated cellulose oligomers synthesized via *in vitro* enzymatic reactions. *Langmuir* **32**, 10120–10125 (2016).
29 Nohara, T., Sawada, T., Tanaka, H. & Serizawa, T. Enzymatic synthesis of oligo(ethylene glycol)-bearing cellulose oligomers for *in situ* formation of hydrogels with crystalline nanoribbon network structures. *Langmuir* **32**, 12520–12526 (2016).
30 Hata, Y., Kojima, T., Koizumi, T., Okura, H., Sakai, T., Sawada, T. & Serizawa, T. Enzymatic synthesis of cellulose oligomer hydrogels composed of crystalline nanoribbon networks under macromolecular crowding conditions. *ACS Macro Lett.* **6**, 165–170 (2017).

31 Breydo, L., Reddy, K. D., Piai, A., Felli, I. C., Pierattelli, R. & Uversky, V. N. The crowd you're in with: effects of different types of crowding agents on protein aggregation. *Biochim. Biophys. Acta* **1844**, 346–357 (2014).
32 Zhang, X., Servos, M. R. & Liu, J. Ultrahigh nanoparticle stability against salt, pH, and solvent with retained surface accessibility via depletion stabilization. *J. Am. Chem. Soc.* **134**, 9910–9913 (2012).
33 Ellis, R. J. Macromolecular crowding: obvious but underappreciated. *Trends Biochem. Sci.* **26**, 597–604 (2001).
34 Lee, C. F., Bird, S., Shaw, M., Jean, L. & Vaux, D. J. Combined effects of agitation, macromolecular crowding, and interfaces on amyloidogenesis. *J. Biol. Chem.* **287**, 38006–38019 (2012).
35 Krishnareddy, M., Kim, Y.-K., Kitaoka, M., Mori, Y. & Hayashi, K. Cellodextrin phosphorylase from *Clostridium thermocellum* YM4 strain expressed in *Escherichia coli*. *J. Appl. Glycosci.* **49**, 1–8 (2002).
36 Homchaudhuri, L., Sarma, N. & Swaminathan, R. Effect of crowding by dextrans and Ficolls on the rate of alkaline phosphatase-catalyzed hydrolysis: a size-dependent investigation. *Biopolymers* **83**, 477–486 (2006).
37 Sasaki, Y., Miyoshi, D. & Sugimoto, N. Effect of molecular crowding on DNA polymerase activity. *Biotechnol. J.* **1**, 440–446 (2006).
38 Nakano, S., Kitagawa, Y., Yamashita, H., Miyoshi, D. & Sugimoto, N. Effects of cosolvents on the folding and catalytic activities of the hammerhead ribozyme. *Chembiochem* **16**, 1803–1810 (2015).
39 Flugge, L. A., Blank, J. T. & Petillo, P. A. Isolation, modification, and NMR assignments of a series of cellulose oligomers. *J. Am. Chem. Soc.* **121**, 7228–7238 (1999).
40 Sugiyama, H., Hisamichi, K., Usui, T., Sakai, K. & Ishiyama, J.-I. A study of the conformation of β-1,4-linked glucose oligomers, cellobiose to cellohexaose, in solution. *J. Mol. Struct.* **556**, 173–177 (2000).
41 Xiong, B., Zhao, P., Cai, P., Zhang, L., Hu, K. & Cheng, G. NMR spectroscopic studies on the mechanism of cellulose dissolution in alkali solutions. *Cellulose* **20**, 613–621 (2013).
42 Samain, E., Lancelon-Pin, C., Férigo, F., Moreau, V., Chanzy, H., Heyraud, A. & Driguez, H. Phosphorolytic synthesis of cellodextrins. *Carbohydr. Res.* **271**, 217–266 (1995).
43 Nakano, S., Miyoshi, D. & Sugimoto, N. Effects of molecular crowding on the structures, interactions, and functions of nucleic acids. *Chem. Rev.* **114**, 2733–2758 (2014).
44 Nelson, M. L. & O'Connor, R. T. Relation of certain infrared bands to cellulose crystallinity and crystal latticed type. Part I. Spectra of lattice types I, II, III and of amorphous cellulose. *J. Appl. Polym. Sci.* **8**, 1311–1324 (1964).